PERGAMON

International Journal of Solids and Structures 38 (2001) 8929–8940

INTERNATIONAL JOURNAL OF SOLIDS and STRUCTURES

www.elsevier.com/locate/ijsolstr

A numerical solution of torsional stress wave propagation in layered orthotropic bar of rectangular cross-section

Liu Kaishin [a,*], Li Bin [b]

[a] *Department of Mechanics and Engineering Sciences, Peking University, Beijing 100871, China*
[b] *Department of Power Engineering, North China Electric Power University, Beijing 102206, China*

Received 22 September 1999

Abstract

A numerical scheme based on the method of numerical integration along bicharacteristics is developed for the numerical analysis of torsional wave propagation in layered orthotropic media. The dynamic behavior of a layered orthotropic bar of rectangular cross-section due to impact torque is studied. Moreover, the stability of the present method is investigated.

Keywords: Stress wave; Orthotropic media; Impact; Numerical analysis; Bicharacteristics

1. Introduction

It has been long recognized that the propagation of stress waves in layered media has important applications in seismology, geophysics and composite structures. A beginning in the field of the transient wave propagation in elastic solid was made by Lamb (1904), then many researchers devote their attention to the transient wave propagation properties in layered isotropic solid (Kennett and Kerry, 1979; Luco and Apsel, 1983; Alterman and Karal, 1968). Moreover, the problems of two-dimensional wave propagation in layered transversely isotropic media were solved by the authors (Liu et al., 1997; Liu and Xie, 1998). Nevertheless very little attention has been paid to the range of three-dimensional wave propagation problem in anisotropic one, just as the case of a bar of noncircular cross-section subjected to impact torque.

In this paper, a numerical algorithm based on the finite difference along bicharacteristics (see e.g. Courant and Hilbert, 1962; Butler, 1960; Clifton, 1967; Ting, 1981) has been proved to be an effective technique for solving the wave propagation problems in layered orthotropic media. The obvious advantage of this method is attributed to the fact that the propagation, reflection and interaction of stress wave in a body can be examined in detail (Lambourn and Hoskin, 1970; Karpp and Chou, 1973). Now, this method is extended to illustrate the three-dimensional torsional wave propagation in a layered orthotropic bar of rectangular cross-section. As for the layered medium, the key problem is of treating the points on the

* Corresponding author. Tel.: +86-10-62765844; fax: +86-10-62751812.
E-mail address: kliu@mech.pku.edu.cn (K. Liu).

0020-7683/01/$ - see front matter
PII: S0020-7683(01)00058-0

interface. Here, we introduce the continuity condition and the available compatibility relation along bi-characteristics to deal with the previous problem, which has been successfully applied to analyzing and numerical simulating the torsional wave propagation in a layered transversely isotropic cylinder (Liu et al., 1997; Liu and Xie, 1998). Moreover, both the von Neumann necessary condition and the relative energy error are taken to investigate the stability in the system.

2. Three-dimensional analysis of torsional waves

Let us consider a rectangular bar, consisting of m layers of orthotropic and homogeneous material, which is subjected to an impact torque on its end surface $z = 0$ and the lateral surfaces are free from external forces (Fig. 1). For the arbitrary layer of the rectangular bar, it is convenient to assume that the planes of the cross-sections of the layered bar maintain to planes of elastic symmetry (the state of stress is pure shear). In consequence, the equations of motion can be written in terms of the Cartesian coordinate system (x, y, z) as

$$\frac{\partial \sigma_{xy}^i}{\partial y} + \frac{\partial \sigma_{zx}^i}{\partial z} = \rho^i \frac{\partial v_x^i}{\partial t}, \tag{1a}$$

$$\frac{\partial \sigma_{xy}^i}{\partial x} + \frac{\partial \sigma_{yz}^i}{\partial z} = \rho^i \frac{\partial v_y^i}{\partial t}, \tag{1b}$$

$$\frac{\partial \sigma_{zx}^i}{\partial x} + \frac{\partial \sigma_{yz}^i}{\partial y} = \rho^i \frac{\partial v_z^i}{\partial t}, \tag{1c}$$

where the superscript i $(i = 1, 2, \ldots, m)$ denotes the layer number of the material, ρ the mass density, σ_{xy}, σ_{yz} and σ_{zx} the stress components, v_x, v_y and v_z the particle velocity components, and t the time. It is further assumed that the deformations and rotations are very small. Therefore, substituting the geometric equation into the physical one yields

$$\frac{\partial \sigma_{yz}^i}{\partial t} = C_{44}^i \left(\frac{\partial v_y^i}{\partial z} + \frac{\partial v_z^i}{\partial y} \right), \tag{2a}$$

$$\frac{\partial \sigma_{zx}^i}{\partial t} = C_{55}^i \left(\frac{\partial v_z^i}{\partial x} + \frac{\partial v_x^i}{\partial z} \right), \tag{2b}$$

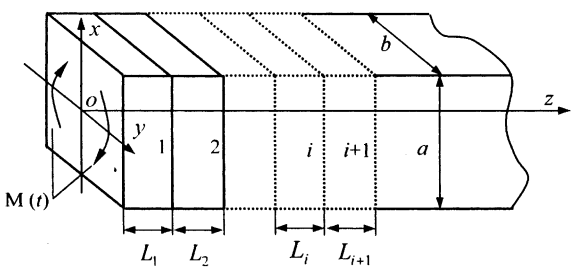

Fig. 1. Semi-infinite layered orthotropic bar of rectangular cross-section and coordinate system.

$$\frac{\partial \sigma_{xy}^i}{\partial t} = C_{66}^i \left(\frac{\partial v_x^i}{\partial y} + \frac{\partial v_y^i}{\partial x} \right), \tag{2c}$$

where C_{44}, C_{55} and C_{66} are elastic coefficients.

The governing equations (1a)–(1c) and (2a)–(2c) can also be expressed in the following matrix form

$$U_{,t}^i = A_x^i U_{,x}^i + A_y^i U_{,y}^i + A_z^i U_{,z}^i, \tag{3}$$

where the vector $U^i = (v_x^i, v_y^i, v_z^i, \sigma_{yz}^i, \sigma_{zx}^i, \sigma_{xy}^i)^T$, $U_{,t}^i$, $U_{,x}^i$, $U_{,y}^i$ and $U_{,z}^i$ are the partial derivatives of U^i with respect to t, x, y and z, respectively, the matrices A_x^i, A_y^i and A_z^i have the following nonzero components

$$A_{x26}^i = A_{x35}^i = A_{y16}^i = A_{y34}^i = A_{z15}^i = A_{z24}^i = \frac{1}{\rho^i},$$

$$A_{x62}^i = A_{y61}^i = C_{66}^i, A_{x53}^i = A_{z51}^i = C_{55}^i, A_{y43}^i = A_{z42}^i = C_{44}^i.$$

The surface $\phi = t - \tau(x,y,z) = 0$ is introduced to represent a characteristic surface in space (x,y,z,t). The value of function $f(x,y,z,t)$ on the characteristic surface can be defined as the following expression by $\overset{*}{f}(x,y,z,\tau(x,y,z))$

$$\overset{*}{f}_{,\alpha} = f_{,\alpha} + f_{,t}\tau_{,\alpha} \quad (\alpha = x,y,z), \tag{4}$$

where $f_{,\alpha}$ and $f_{,t}$ present the values on the characteristic surface after taking the partial differentiation. When formula (4) is substituted for stresses and velocities in Eq. (3), the following matrix form can be obtained

$$DV_{,t} + A = 0, \tag{5}$$

where

$$V_{,t} = \begin{bmatrix} \frac{\partial v_x^i}{\partial t} \\ \frac{\partial v_y^i}{\partial t} \\ \frac{\partial v_z^i}{\partial t} \end{bmatrix}, \quad D = \begin{bmatrix} C_{66}^i \tau_{,y}^2 + C_{55}^i \tau_{,z}^2 - \rho^i & C_{66}^i \tau_{,x}\tau_{,y} & C_{55}^i \tau_{,x}\tau_{,z} \\ C_{66}^i \tau_{,x}\tau_{,y} & C_{66}^i \tau_{,x}^2 + C_{44}^i \tau_{,z}^2 - \rho^i & C_{44}^i \tau_{,y}\tau_{,z} \\ C_{55}^i \tau_{,x}\tau_{,z} & C_{44}^i \tau_{,y}\tau_{,z} & C_{55}^i \tau_{,x}^2 + C_{44}^i \tau_{,y}^2 - \rho^i \end{bmatrix},$$

$$A = \begin{bmatrix} \overset{*}{\sigma}_{xy,y}^i + \overset{*}{\sigma}_{zx,z}^i - C_{66}^i \tau_{,y} \left(\overset{*}{v}_{x,y}^i + \overset{*}{v}_{y,x}^i \right) - C_{55}^i \tau_{,z} \left(\overset{*}{v}_{x,z}^i + \overset{*}{v}_{z,x}^i \right) \\ \overset{*}{\sigma}_{xy,x}^i + \overset{*}{\sigma}_{yz,z}^i - C_{66}^i \tau_{,x} \left(\overset{*}{v}_{x,y}^i + \overset{*}{v}_{y,x}^i \right) - C_{44}^i \tau_{,z} \left(\overset{*}{v}_{y,z}^i + \overset{*}{v}_{z,y}^i \right) \\ \overset{*}{\sigma}_{zx,x}^i + \overset{*}{\sigma}_{yz,y}^i - C_{55}^i \tau_{,x} \left(\overset{*}{v}_{x,z}^i + \overset{*}{v}_{z,x}^i \right) - C_{44}^i \tau_{,y} \left(\overset{*}{v}_{y,z}^i + \overset{*}{v}_{z,y}^i \right) \end{bmatrix}.$$

The differential equation of the characteristic surface is governed by

$$\text{Det } D = 0. \tag{6}$$

For a certain time t, let $n = (n_x, n_y, n_z)$ be the unit normal vector to the characteristic surface, and c^i the normal wave speed. Then we have

$$\tau_{,\alpha} = \frac{n_\alpha}{c^i} \quad (\alpha = x,y,z). \tag{7}$$

The bicharacteristics of Eq. (5), which are equivalent to the characteristics of Eq. (6), are

$$\frac{\mathrm{d}\alpha}{\mathrm{d}t} = c^i n_\alpha \quad (\alpha = x, y, z). \tag{8}$$

The total differentiation of a function $f(x, y, z, t)$ along a bicharacteristic is given by

$$\frac{\mathrm{d}f}{\mathrm{d}t} = c^i (f_{,x} n_x + f_{,y} n_y + f_{,z} n_z) + f_{,t}. \tag{9}$$

Eliminating $f_{,t}$ between Eqs. (4) and (9) leads to the following expression

$$\overset{*}{f}{}^i_{,\alpha} = \frac{\mathrm{d}f}{\mathrm{d}t}\tau_{,t} + f_{,\alpha} - c^i \tau_{,t}(f_{,x} n_x + f_{,y} n_y + f_{,z} n_z), \quad (\alpha = x, y, z). \tag{10}$$

There exists a left eigenvectors $l(= l_1, l_2, l_3)$, which makes the following expression

$$lD = 0. \tag{11}$$

It is easily obtained the following equation

$$l(DV_{,t} + A) = 0. \tag{12}$$

By using Eqs. (8)–(11), Eq. (12) can be converted into

$$\begin{aligned}
&\frac{\mathrm{d}\sigma^i_{xy}}{\mathrm{d}t}(l_1 n_y + l_2 n_x) + \frac{\mathrm{d}\sigma^i_{yz}}{\mathrm{d}t}(l_2 n_z + l_3 n_y) + \frac{\mathrm{d}\sigma^i_{zx}}{\mathrm{d}t}(l_1 n_z + l_3 n_x) - \frac{\mathrm{d}v^i_x}{\mathrm{d}t}\left[\left(\frac{C^i_{66}}{c^i} n_y^2 + \frac{C^i_{55}}{c^i} n_z^2\right) l_1 \right.\\
&\quad \left. + \frac{C^i_{66}}{c^i} n_x n_y l_2 + \frac{C^i_{55}}{c^i} n_x n_z l_3\right] - \frac{\mathrm{d}v^i_y}{\mathrm{d}t}\left[\left(\frac{C^i_{66}}{c^i} n_x^2 + \frac{C^i_{44}}{c^i} n_z^2\right) l_2 + \frac{C^i_{66}}{c^i} n_x n_y l_1 + \frac{C^i_{44}}{c^i} n_y n_z l_3\right]\\
&\quad - \frac{\mathrm{d}v^i_z}{\mathrm{d}t}\left[\left(\frac{C^i_{55}}{c^i} n_x^2 + \frac{C^i_{44}}{c^i} n_y^2\right) l_3 + \frac{C^i_{55}}{c^i} n_x n_z l_1 + \frac{C^i_{44}}{c^i} n_y n_z l_2\right] = -S,
\end{aligned} \tag{13}$$

where

$$\begin{aligned}
S = {} & c^i l_1(\sigma^i_{xy,y} + \sigma^i_{zx,z}) + c^i l_2(\sigma^i_{xy,x} + \sigma^i_{yz,z}) + c^i l_3(\sigma^i_{zx,x} + \sigma^i_{yz,y}) - C^i_{66}(n_y l_1 + n_x l_2)(v^i_{x,y} + v^i_{y,x})\\
& - C^i_{55}(n_z l_1 + n_x l_3)(v^i_{x,z} + v^i_{z,x}) - C^i_{44}(n_z l_2 + n_y l_3)(v^i_{y,z} + v^i_{z,y}) - c^i(n_y l_1 + n_x l_2)(\sigma^i_{xy,x} n_x + \sigma^i_{xy,y} n_y + \sigma^i_{xy,z} n_z)\\
& - c(n_z l_1 + n_x l_3)(\sigma_{zx,x} n_x + \sigma_{zx,y} n_y + \sigma_{zx,z} n_z) - c(n_z l_2 + n_y l_3)(\sigma_{yz,x} n_x + \sigma_{yz,y} n_y + \sigma_{yz,z} n_z)\\
& + \left[C^i_{66}(l_1 n_y^2 + l_2 n_x n_y) + C^i_{55}(l_1 n_z^2 + l_3 n_x n_z)\right](v^i_{x,x} n_x + v^i_{x,y} n_y + v^i_{x,z} n_z)\\
& + \left[C^i_{66}(l_2 n_x^2 + l_1 n_x n_y) + C^i_{44}(l_2 n_z^2 + l_3 n_y n_z)\right](v^i_{y,x} n_x + v^i_{y,y} n_y + v^i_{y,z} n_z)\\
& + \left[C^i_{55}(l_3 n_x^2 + l_1 n_x n_z) + C^i_{44}(l_3 n_y^2 + l_2 n_y n_z)\right](v^i_{z,x} n_x + v^i_{z,y} n_y + v^i_{z,z} n_z).
\end{aligned}$$

In order to get the numerical solution by the method of numerical integration along bicharacteristics, it is convenient to select the bicharacteristics on the surfaces $x = 0$, $y = 0$ and $z = 0$. So the solutions of Eq. (11) may be given as

$$
\begin{aligned}
c_1^i &= \sqrt{C_{66}^i/\rho^i} \quad \text{for} \quad n=(\pm1,0,0),\ \ l=(0,1,0),\\
c_2^i &= \sqrt{C_{55}^i/\rho^i} \quad \text{for} \quad n=(\pm1,0,0),\ \ l=(0,0,1),\\
c_1^i &= \sqrt{C_{66}^i/\rho^i} \quad \text{for} \quad n=(0,\pm1,0),\ \ l=(1,0,0),\\
c_3^i &= \sqrt{C_{44}^i/\rho^i} \quad \text{for} \quad n=(0,\pm1,0),\ \ l=(0,0,1),\\
c_2^i &= \sqrt{C_{55}^i/\rho^i} \quad \text{for} \quad n=(0,0,\pm1),\ \ l=(1,0,0),\\
c_3^i &= \sqrt{C_{44}^i/\rho^i} \quad \text{for} \quad n=(0,0,\pm1),\ \ l=(0,1,0).
\end{aligned}
$$

Substituting the above values into Eq. (13), the differential relations along bicharacteristics may be written as

$$
\begin{aligned}
&\frac{\mathrm{d}\sigma_{xy}^i}{\mathrm{d}t}-\rho^i c_1^i\frac{\mathrm{d}v_y^i}{\mathrm{d}t}=-c_1^i\sigma_{yz,z}^i+\rho^i\left(c_1^i\right)^2 v_{x,y}^i \quad \text{for } c^i=c_1^i,\ \ l=(0,1,0),\\
&\frac{\mathrm{d}\sigma_{xy}^i}{\mathrm{d}t}+\rho^i c_1^i\frac{\mathrm{d}v_y^i}{\mathrm{d}t}=c_1^i\sigma_{yz,z}^i+\rho^i\left(c_1^i\right)^2 v_{x,y}^i \quad \text{for } c^i=-c_1^i,\ \ l=(0,1,0),\\
&\frac{\mathrm{d}\sigma_{zx}^i}{\mathrm{d}t}-\rho^i c_2^i\frac{\mathrm{d}v_z^i}{\mathrm{d}t}=-c_2^i\sigma_{yz,y}^i+\rho^i\left(c_2^i\right)^2 v_{x,z}^i \quad \text{for } c^i=c_2^i,\ \ l=(0,0,1),\\
&\frac{\mathrm{d}\sigma_{zx}^i}{\mathrm{d}t}+\rho^i c_2^i\frac{\mathrm{d}v_z^i}{\mathrm{d}t}=c_2^i\sigma_{yz,y}^i+\rho^i\left(c_2^i\right)^2 v_{x,z}^i \quad \text{for } c^i=-c_2^i,\ \ l=(0,0,1),\\
&\frac{\mathrm{d}\sigma_{xy}^i}{\mathrm{d}t}-\rho^i c_1^i\frac{\mathrm{d}v_x^i}{\mathrm{d}t}=-c_1^i\sigma_{zx,z}^i+\rho^i\left(c_1^i\right)^2 v_{y,x}^i \quad \text{for } c^i=c_1^i,\ \ l=(1,0,0),\\
&\frac{\mathrm{d}\sigma_{xy}^i}{\mathrm{d}t}+\rho^i c_1^i\frac{\mathrm{d}v_x^i}{\mathrm{d}t}=c_1^i c_{zx,z}^i+\rho^i\left(c_1^i\right)^2 v_{y,x}^i \quad \text{for } c^i=-c_1^i,\ \ l=(1,0,0),\\
&\frac{\mathrm{d}\sigma_{yz}^i}{\mathrm{d}t}-\rho^i c_3^i\frac{\mathrm{d}v_z^i}{\mathrm{d}t}=-c_3^i\sigma_{zx,x}^i+\rho^i\left(c_3^i\right)^2 v_{y,z}^i \quad \text{for } c^i=c_3^i,\ \ l=(0,0,1),\\
&\frac{\mathrm{d}\sigma_{yz}^i}{\mathrm{d}t}+\rho^i c_3^i\frac{\mathrm{d}v_z^i}{\mathrm{d}t}=c_3^i\sigma_{zx,x}^i+\rho^i\left(c_3^i\right)^2 v_{y,z}^i \quad \text{for } c^i=-c_3^i,\ \ l=(0,0,1),\\
&\frac{\mathrm{d}\sigma_{zx}^i}{\mathrm{d}t}-\rho^i c_2^i\frac{\mathrm{d}v_x^i}{\mathrm{d}t}=-c_2^i\sigma_{xy,y}^i+\rho^i\left(c_2^i\right)^2 v_{z,x}^i \quad \text{for } c^i=c_2^i,\ \ l=(1,0,0),\\
&\frac{\mathrm{d}\sigma_{zx}^i}{\mathrm{d}t}+\rho^i c_2^i\frac{\mathrm{d}v_x^i}{\mathrm{d}t}=c_2^i\sigma_{xy,y}^i+\rho^i\left(c_2^i\right)^2 v_{z,x}^i \quad \text{for } c^i=-c_2^i,\ \ l=(1,0,0),\\
&\frac{\mathrm{d}\sigma_{yz}^i}{\mathrm{d}t}-\rho^i c_3^i\frac{\mathrm{d}v_y^i}{\mathrm{d}t}=-c_3^i\sigma_{xy,x}^i+\rho^i\left(c_3^i\right)^2 v_{z,y}^i \quad \text{for } c^i=c_3^i,\ \ l=(0,1,0),\\
&\frac{\mathrm{d}\sigma_{yz}^i}{\mathrm{d}t}+\rho^i c_3^i\frac{\mathrm{d}v_y^i}{\mathrm{d}t}=c_3^i\sigma_{xy,x}^i+\rho^i\left(c_3^i\right)^2 v_{z,y}^i \quad \text{for } c^i=-c_3^i,\ \ l=(0,1,0).
\end{aligned}
\tag{14}
$$

Integrating Eq. (14) along the corresponding bicharacteristics and Eq. (5) along the time axis, and performing proper linear combinations of those equations, we can successively obtain the following differential relations for six unknown increments

$$
\begin{aligned}
\delta v_x^i &= \frac{(c_2^i)^2 k}{2C_{55}^i}\left[2(\sigma_{xy,x}^i+\sigma_{zx,z}^i)+(v_{y,xy}^i+v_{x,yy}^i)C_{66}^i k+(v_{z,zx}^i+v_{x,zz}^i)C_{55}^i k\right]+\mathrm{O}(k^3),\\
\delta v_y^i &= \frac{(c_3^i)^2 k}{2C_{44}^i}\left[2(\sigma_{xy,x}^i+\sigma_{yz,z}^i)+(v_{y,xx}^i+v_{x,xy}^i)C_{66}^i k+(v_{z,zy}^i+v_{y,zz}^i)C_{44}^i k\right]+\mathrm{O}(k^3),\\
\delta v_z^i &= \frac{(c_3^i)^2 k}{2C_{44}^i}\left[2(\sigma_{zx,x}^i+\sigma_{yz,y}^i)+(v_{z,xx}^i+v_{x,xz}^i)C_{55}^i k+(v_{z,yy}^i+v_{y,yz}^i)C_{44}^i k\right]+\mathrm{O}(k^3),\\
\delta\sigma_{xy}^i &= \frac{k}{2}\left[2C_{66}^i(v_{y,x}^i+v_{x,y}^i)+(\sigma_{xy,xx}^i+\sigma_{yz,xz}^i+\sigma_{xy,yy}^i+\sigma_{zx,yz}^i)(c_1^i)^2 k\right]+\mathrm{O}(k^3),\\
\delta\sigma_{yz}^i &= \frac{k}{2}\left[2C_{44}^i(v_{z,y}^i+v_{y,z}^i)+(\sigma_{zx,xy}^i+\sigma_{yz,yy}^i+\sigma_{xy,zx}^i+\sigma_{yz,zz}^i)(c_3^i)^2 k\right]+\mathrm{O}(k^3),\\
\delta\sigma_{zx}^i &= \frac{k}{2}\left[2C_{55}^i(v_{z,x}^i+v_{x,z}^i)+(\sigma_{zx,xx}^i+\sigma_{yz,xy}^i+\sigma_{xy,zy}^i+\sigma_{zx,zz}^i)(c_2^i)^2 k\right]+\mathrm{O}(k^3),
\end{aligned}
\tag{15}
$$

where $\delta f = f(x_0,y_0,z_0,t_0)-f(x_0,y_0,z_0,t_0-k)$, k is the time step, (x_0,y_0,z_0,t_0) is an arbitrary point in space time. The quantities on the right-hand side of Eq. (15) are all known data at the point (x_0,y_0,z_0,t_0-k), and the partial differences $f_{,x}$, $f_{,y}$, $f_{,z}$, $f_{,xx}$, $f_{,yy}$, $f_{,zz}$, $f_{,xy}$, $f_{,yz}$ and $f_{,zx}$ at the point(x_0,y_0,z_0,t_0-k) can be approximated by central differences.

When the point (x_0,y_0,z_0,t_0) is located on the interface between layers i and $i+1$, the bicharacteristics corresponding to $n=(0,0,-1)$ for layer i and $n=(0,0,1)$ for layer $i+1$, which all intersect the plane $t=t_0-k$ at points in their adjacent layers, should not be employed in the computation of the unknown increments. On the interface between the two layers, the following velocity and stress components must be continuous

$$
v_x^i = v_x^{i+1},\quad v_y^i = v_y^{i+1},\quad v_z^i = v_z^{i+1},\quad \sigma_{yz}^i = \sigma_{yz}^{i+1},\quad \sigma_{zx}^i = \sigma_{zx}^{i+1}. \tag{16}
$$

Using the similar way for obtaining Eq. (15), we can finally obtain the following unknown velocity and stress components with the help of Eq. (16):

$$
\begin{aligned}
\delta v_x^i &= \delta v_x^{i+1} = \frac{D_3-D_4}{A_2+B_2},\\
\delta v_y^i &= \delta v_y^{i+1} = \frac{D_1-D_2}{A_1+B_1},\\
\delta v_z^i &= \delta v_z^{i+1} = \frac{D_5}{A_3},\\
\delta\sigma_{yz}^i &= \delta\sigma_{yz}^{i+1} = \frac{A_1D_2+B_1D_1}{A_1+B_1},\\
\delta\sigma_{zx}^i &= \delta\sigma_{zx}^{i+1} = \frac{A_2D_4+B_2D_3}{A_2+B_2},\\
\delta\sigma_{xy}^i &= \frac{k}{2}\left[2C_{66}^i\left(v_{y,x}^i+v_{x,y}^i\right)+(c_1^i)^2 k\left(\sigma_{xy,xx}^i+\sigma_{xy,yy}^i+\sigma_{zx,yz}^i+\sigma_{yz,zx}^i\right)\right],\\
\delta\sigma_{xy}^{i+1} &= \frac{k}{2}\left[2C_{66}^{i+1}\left(v_{y,x}^{i+1}+v_{x,y}^{i+1}\right)+(c_1^{i+1})^2 k\left(\sigma_{xy,xx}^{i+1}+\sigma_{xy,yy}^{i+1}+\sigma_{zx,yz}^{i+1}+\sigma_{yz,zx}^{i+1}\right)\right],
\end{aligned}
\tag{17}
$$

where

$$A_1 = \frac{C_{44}^i}{c_3^i}, \quad A_2 = \frac{C_{55}^i}{c_2^i}, \quad A_3 = \frac{2C_{55}^i}{(c_2^i)^2} + \frac{C_{55}^{i+1}}{(c_2^{i+1})^2},$$

$$B_1 = \frac{C_{44}^{i+1}}{c_3^{i+1}}, \quad B_2 = \frac{C_{55}^{i+1}}{c_2^{i+1}},$$

$$D_1 = \frac{kc_3^i}{(c_2^i)^2}\Big\langle (c_2^i)^2\Big\{\Big[2\Big(\sigma_{xy,x}^i + \sigma_{yz,z}^i\Big) + C_{66}^i k\Big(v_{y,xx}^i + v_{x,xy}^i\Big)\Big] - c_3^i k\Big(\sigma_{zx,xy}^i + \sigma_{yz,yy}^i + \sigma_{xy,zx}^i + \sigma_{yz,zz}^i\Big)\Big\}$$
$$- 2c_3^i C_{55}^i\Big(v_{z,y}^i + v_{y,z}^i\Big) + (c_3^i)^2 C_{55}^i k\Big(v_{z,yz}^i + v_{y,zz}^i\Big)\Big\rangle,$$

$$D_2 = -\frac{k}{2}\Big\langle c_3^{i+1} k\Big\{\Big[C_{66}^{i+1}\Big(v_{y,xx}^{i+1} + v_{x,xy}^{i+1}\Big) + C_{44}^{i+1}\Big(v_{z,yz}^{i+1} + v_{y,zz}^{i+1}\Big)\Big] + c_3^{i+1}\Big(\sigma_{zx,xy}^{i+1} + \sigma_{yz,yy}^{i+1} + \sigma_{xy,zx}^{i+1} + \sigma_{yz,zz}^{i+1}\Big)\Big\}$$
$$+ 2\Big[c_3^{i+1}\Big(\sigma_{xy,x}^{i+1} + \sigma_{yz,z}^{i+1}\Big) + C_{44}^{i+1}\Big(v_{z,y}^{i+1} + v_{y,z}^{i+1}\Big)\Big]\Big\rangle,$$

$$D_3 = \frac{k}{2}\Big\{c_2^i\Big[C_{66}^i k\Big(v_{y,xy}^i + v_{x,yy}^i\Big) + C_{55}^i k\Big(v_{z,zx}^i + v_{x,zz}^i\Big) + 2\Big(\sigma_{xy,y}^i + \sigma_{zx,z}^i\Big)\Big] - 2C_{55}^i\Big(v_{z,x}^i + v_{x,z}^i\Big)$$
$$- (c_2^i)^2 k\Big(\sigma_{zx,xx}^i + \sigma_{yz,xy}^i + \sigma_{xy,yz}^i + \sigma_{zx,zz}^i\Big)\Big\},$$

$$D_4 = -\frac{k}{2}\Big\langle c_2^{i+1} k\Big\{\Big[C_{66}^{i+1}\Big(v_{y,xy}^{i+1} + v_{x,yy}^{i+1}\Big) + C_{55}^{i+1}\Big(v_{z,zx}^{i+1} + v_{x,zz}^{i+1}\Big)\Big] + c_2^{i+1}\Big(\sigma_{zx,xx}^{i+1} + \sigma_{yz,xy}^{i+1} + \sigma_{xy,yz}^{i+1} + \sigma_{zx,zz}^{i+1}\Big)\Big\}$$
$$+ 2\Big[C_{55}^{i+1}\Big(v_{z,x}^{i+1} + v_{x,z}^{i+1}\Big) + c_2^{i+1}\Big(\sigma_{xy,y}^{i+1} + \sigma_{zx,z}^{i+1}\Big)\Big]\Big\rangle,$$

$$D_5 = \frac{k}{2(c_2^i)^2}\Big\{(c_2^i)^2\Big[\Big(\sigma_{zx,x}^{i+1} + \sigma_{yz,y}^{i+1} - 3\sigma_{zx,x}^i - 3\sigma_{yz,y}^i\Big) - C_{55}^i k\Big(v_{z,xx}^i + v_{x,zx}^i\Big)\Big] - (c_3^i)^2 C_{55}^i k\Big(v_{z,yy}^i + v_{y,yz}^i\Big)\Big\}.$$

When the point$(x_0, y_0, z_0, t_0 - k)$ is located on the boundary, some bicharacteristics on the characteristic surface intersect the plane $t = t_0 - k$ at points outside the region of interest. Therefore, the relations along those bicharacteristics cannot be used. Instead of those unused relations, the admissible boundary conditions are adopted to work out the numerical solution at the point located on the boundary. Simultaneously, the forward or backward difference equations should be employed for approximating the partial differentiation.

3. Numerical simulation

In order to generalize the features of the three-dimensional torsional stress wave propagation in layered orthotropic rectangular bar, we calculate several numerical examples simulating stress wave propagation in a semi-infinite two-layer rectangular bar with different materials on the basis of the numerical method described in the present paper.

Assuming the planes of the cross-sections are planes of elastic symmetry and referring the analysis result (Lekhnitskii, 1981) for the same rectangular bar loading a static toque, we take the initial and boundary conditions as

$$\begin{aligned}
&\sigma_{xy}^i = \sigma_{yz}^i = \sigma_{zx}^i = v_x^i = v_y^i = v_z^i = 0, \quad (i = 1, 2) \text{ for } t = 0,\\
&\sigma_{yz}^i = p_1(t),\ \sigma_{zx}^i = p_2(t),\ \sigma_{xy}^i = 0, \quad (i = 1) \text{ for } z = 0,\\
&\sigma_{xy}^i = \sigma_{zx}^i = 0, \quad (i = 1, 2) \text{ for } x = \pm\frac{a}{2},\\
&\sigma_{xy}^i = \sigma_{yz}^i = 0, \quad (i = 1, 2) \text{ for } y = \pm\frac{b}{2},
\end{aligned} \tag{18a}$$

where

$$p_1(t) = \frac{8M(t)}{b^3\mu^2\pi^2\beta}\sum_{m=1,3,5,\ldots}^{\infty}\frac{1}{m^2}(-1)^{(m-1/2)}\left(1-\frac{\cosh(m\pi\mu y/a)}{\cosh(m\pi\mu/2\gamma)}\right)\sin\frac{m\pi x}{a},$$
$$p_2(t) = -\frac{8M(t)}{b^3\pi^2\mu\beta}\sum_{m=1,3,5,\ldots}^{\infty}\frac{1}{m^2}(-1)^{(m-1/2)}\left(\frac{\sinh(m\pi\mu y/a)}{\cosh(m\pi\mu/2\gamma)}\right)\cos\frac{m\pi x}{a}, \tag{18b}$$

in which a and b are the depth and width of the rectangular cross-section, $\gamma = a/b$ the ratio of lateral dimension, $\mu = \sqrt{C_{44}^1/C_{55}^1}$ the ratio of elastic coefficient, the factor β is defined by the series

$$\beta = \frac{32\gamma^2}{\mu^2\pi^4}\sum_{m=1,3,5,\ldots}^{\infty}\frac{1}{m^4}\left(1-\frac{2\gamma\tanh(m\pi\mu/\gamma)}{m\pi\mu}\right),$$

the impact torque $M(t)$ is given by

$$M(t) = \begin{cases}\frac{M_0 t}{t_r}, & \text{for } t \leqslant t_r,\\ M_0, & \text{for } t > t_r,\end{cases} \tag{18c}$$

where $M_0 = 10$ N m, $t_r = 3.454$ μs.

The material and geometric parameters of layer A ($i = 1$) are: $C_{44} = 4.02$ GPa, $C_{55} = 4.41$ GPa, $C_{66} = 4.90$ GPa, $\rho = 2.11 \times 10^3$ kg/m^3, $L_1 = 50$ mm; and the parameters of layer B ($i = 2$) are: $C_{44} = 1.3$ GPa, $C_{55} = 1.3$ GPa, $C_{66} = 1.3$ GPa, $\rho = 1.21 \times 10^3$ kg/m^3, $b = 10$ mm, $L_2 = \infty$. For the two layers, the same spatial mesh size is taken as $h = 0.5$ mm, the same time step size $k = 0.5\ h/c_1$.

The distributions of the shear stress in layer A before the torsional wave reach the interface are investigated first. As a result, we notice that for the impact torque $M(t)$ presented in Eq. (18c), the cross-section of the rectangular bar does not remain plane and the distributions of the torsional stresses become uniform when the wave front passed, which are similar to the case of the rectangular bar under a static torque M_0 (the figures are omitted here) (see e.g. Lekhnitskii, 1981).

Fig. 2 shows the distributions of the shear stress σ_{yz} along the longitudinal line ($x = a/2$, $y = 0$) of a rectangular bar ($\gamma = 1.5$, $\mu = 0.95$) at different times. The symbols I and R located on the ordinate axis in this figure represent the amplitudes of the incident torsional wave and the reflected torsional wave, respectively. From this figure, we can clearly notice that the reflected torsional wave and the transmitted wave occurred on the interface ($z = 50$ mm). Moreover, the amplitude of the shear stress σ_{yz} decreased when the

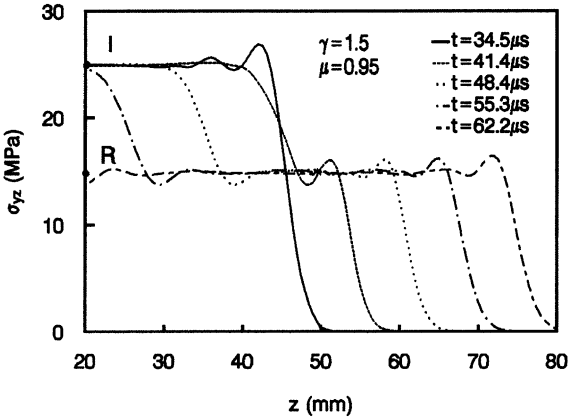

Fig. 2. Distribution of the shear stress σ_{yz} along the longitudinal line ($x = a/2$, $y = 0$) of the rectangular bar ($\gamma = 1.5$, $\mu = 0.95$).

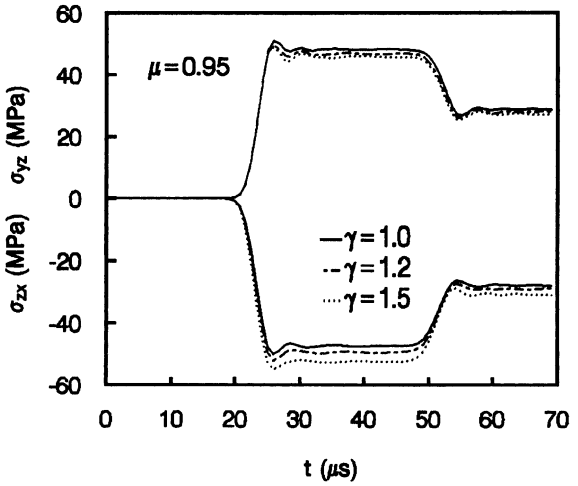

Fig. 3. Shear stress σ_{yz} at the point $(a/2, 0, 3b/2)$ and σ_{zx} at the point $(0, b/2, 3b/2)$ of the rectangular bar with the different ratio γ.

reflected torsional wave passed. It is because that the sign of the shear stress σ_{yz} produced by the reflected torsional wave is opposite to the one produced by the incident torsional wave. At the same time, the distribution of the torsional stress σ_{yz} becomes uniform when the torsional wave front passed.

Fig. 3 describes the time variations of the shear stress σ_{yz} at the point $(a/2, 0, 3b/2)$ and the shear stress σ_{zx} at the point $(0, b/2, 3b/2)$ with the different ratio γ. It can be seen that the amplitude of the shear stress σ_{yz} becomes smaller as the ratio γ rises. But the tendency of the shear stress σ_{zx} with the ratio γ is quite the reverse. In order to clarify the influences of the elastic coefficient ratio μ on the torsional stresses, additional cases are worked out. Fig. 4 shows the time variations of the shear stress σ_{yz} at the point $(a/2, 0, 3b/2)$ and the shear stress σ_{zx} at the point $(0, b/2, 3b/2)$ with the different elastic coefficient ratio μ (where C_{55} maintain constant). From Fig. 5, we can see that the amplitude of the shear stress σ_{yz} increases with the elastic coefficient ratio μ decreasing, while the amplitude of the shear stress σ_{zx} has little changes. The same

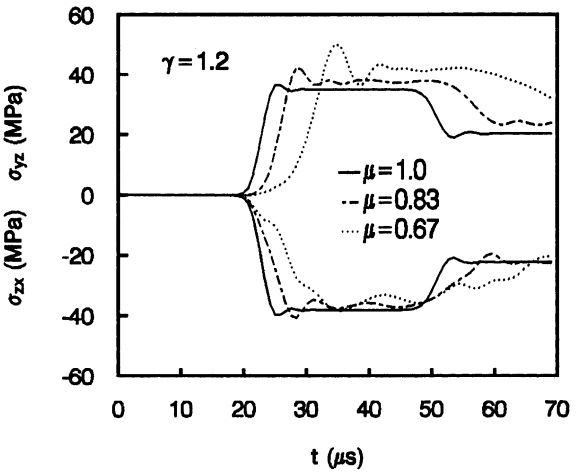

Fig. 4. Shear stress σ_{yz} at the point $(a/2, 0, 3b/2)$ and σ_{zx} at the point $(0, b/2, 3b/2)$ of the rectangular bar with the different elastic coefficient ratio μ.

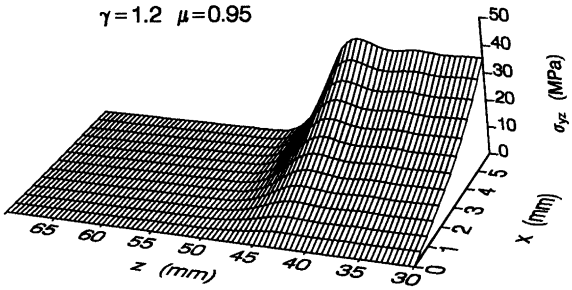

Fig. 5. Distribution of the shear stress σ_{yz} in x–z section of the rectangular bar at time $t = 34.54$ μs.

tendency of the time variations of the shear stresses with γ or μ occurred at the other points of the rectangular bar (its figures are omitted).

The process of the torsional stress wave propagation in the section $y = 0$ of a rectangular bar ($\gamma = 1.2$, $\mu = 0.95$) from layer A into layer B is clearly described by Figs. 5–7. It is evident that the variation of the shear stress distribution at the solid surface near the interface is similar with the case of the layered cylinders (Liu and Xie, 1998).

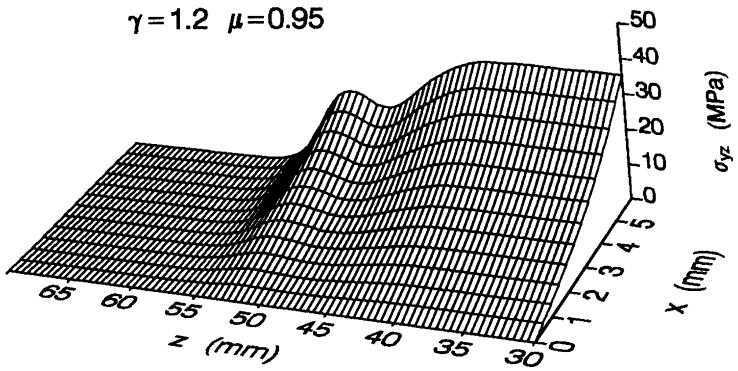

Fig. 6. Distribution of the shear stress σ_{yz} in x–z section of the rectangular bar at time $t = 41.45$ μs.

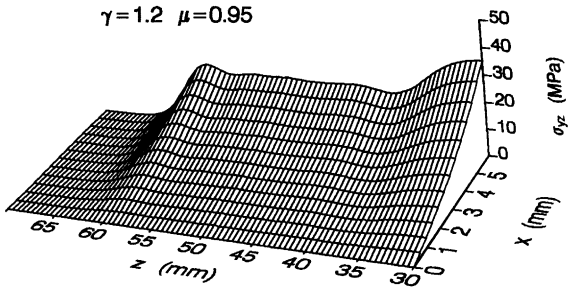

Fig. 7. Distribution of the shear stress σ_{yz} in x–z section of the rectangular bar at time $t = 48.34$ μs.

4. Stability of the difference equations

Instead of making a theoretical investigation of the stability and convergence of the numerical solution, we just obtain an approximate result by taking the von Neumann necessary condition that the spectral radius of the matrix be not greater than unity. It is easily to confirm that Eq. (15) are equivalent to the Lax–Wendroff difference equations for Eq. (3). For this case, by applying Fourier analysis to Eq. (3), the corresponding amplification matrix associated with Eq. (15) can be derived as follows

$$S(\theta_1,\theta_2,\theta_3) = R + \mathrm{i}J \tag{19}$$

with

$$R = I + \left(\frac{k}{h}\right)^2\left[\left(A_x^i\right)^2(\cos\theta_1 - 1) + \left(A_y^i\right)^2(\cos\theta_2 - 1) + \left(A_z^i\right)^2(\cos\theta_3 - 1)\right]$$
$$-\frac{1}{2}\left(\frac{k}{h}\right)^2\left[\left(A_x^iA_y^i + A_y^iA_x^i\right)\sin\theta_1\sin\theta_2 + \left(A_y^iA_z^i + A_z^iA_y^i\right)\sin\theta_2\sin\theta_3 + \left(A_x^iA_z^i + A_z^iA_x^i\right)\sin\theta_1\sin\theta_3\right],$$

$$J = -\frac{k}{h}\left(A_x^i\sin\theta_1 + A_y^i\sin\theta_2 + A_z^i\sin\theta_3\right),$$

where θ_1, θ_2 and θ_3 are arbitrary parameters that correspond to arbitrary wavelengths in the x, y and z directions, I the unit matrix. For the strongest restriction on k/h that ensures satisfaction of the von Neumann necessary condition is $\theta_1 = \theta_2 = \theta_3 = \pi$, the condition for spectral radius of S less than or equal to unity is

$$\left(\frac{c_1^ik}{h}\right)^2 \leqslant \min\left[\frac{C_{66}^i}{C_{66}^i + C_{55}^i}, \frac{C_{66}^i}{C_{44}^i + C_{66}^i}, \frac{C_{66}^i}{C_{44}^i + C_{55}^i}, \frac{1}{2}, \frac{C_{66}^i}{2C_{55}^i}, \frac{C_{66}^i}{2C_{44}^i}\right]. \tag{20}$$

Although the stability analysis described above does not concern the effect of boundary condition, Eq. (20) is very available for selecting the appropriate value of c_1k/h. In fact, the stability of the numerical procedure in the present calculations is checked by evaluating the relative energy error E_{rr} in the system, where E_{rr} is defined as

$$E_{\mathrm{rr}} = \frac{E_{\mathrm{input}} - E_{\mathrm{total}}}{E_{\mathrm{input}}},$$

in which the input energy E_{input} and the total energy E_{total} are evaluated by

$$E_{\mathrm{input}} = \int_{-a/2}^{a/2}\int_{-b/2}^{b/2}\int_0^t(-v_x\sigma_{zx} - v_y\sigma_{yz})\,\mathrm{d}x\,\mathrm{d}y\,\mathrm{d}t,$$

$$E_{\mathrm{total}} = \sum_{i=1}^{m}\int_{-a/2}^{a/2}\int_{-b/2}^{b/2}\int_0^{L_i}\left\{\frac{1}{2}\rho\left[\left(v_x^i\right)^2 + \left(v_y^i\right)^2 + \left(v_z^i\right)^2\right] + \frac{\left(\sigma_{xy}^i\right)^2}{2C_{66}^i} + \frac{\left(\sigma_{yz}^i\right)^2}{2C_{44}^i} + \frac{\left(\sigma_{zx}^i\right)^2}{2C_{55}^i}\right\}\mathrm{d}x\,\mathrm{d}y\,\mathrm{d}z.$$

From Eq. (20), we take $c_1k/h = 0.5$. The numerical tests indicated that the maximum relative energy errors involved in the computed examples were always less than about 0.86%.

5. Conclusion

With the purpose of analyzing torsional stress wave propagation in layered orthotropic media due to impact torque, the numerical algorithm based on the method of numerical integration along bicharacteristics

is proposed. By the numerical examples, the propagation, reflection and transmission of the torsional stress wave in the vicinity of the interface of layered orthotropic bars of rectangular cross-section are examined in detail.

Theoretically, the numerical algorithm developed here is applicable to a wide variety of problems for simulating torsional stress wave propagation in layered orthotropic solids. However, in view of the fact that the treatment for general curved boundaries and interfaces is difficult using the present technique, the computer program is only made for analyzing the impact problems of which the computational model is shown in Fig. 1.

Acknowledgements

This work was supported by the National Natural Science Foundation of China (grant nos.19872015 and 10025212).

References

Alterman, Z., Karal, F.C., 1968. Propagation of elastic waves in layered media by finite different methods. Bull. Seismol. Soc. Am. 58, 367–398.

Butler, D.S., 1960. The numerical solution of hyperbolic systems of partial equations in three independent variables. Proc. R. Soc. A 255, 232–252.

Clifton, R.J., 1967. A difference method for plane problems in dynamic elasticity. Quart. Appl. Math. 25, 97–116.

Courant, R., Hilbert, D., 1962. Methods of Mathematical Physics II. Interscience Publishers, New York.

Karpp, R., Chou, P.C., 1973. Dynamic response of materials to intense impulsive loading. In: Chou, P.C., Hopkins, A.K. (Eds.), The Method of Charecteristics. US Government Printing Office. pp. 287–362.

Kennett, B.L.N., Kerry, N.J., 1979. Seismic waves in a stratified half space. Geophy. J. R. Astr. Soc. 57, 557–583.

Lambourn, B.D., Hoskin, N.E., 1970. The computation of general problems in one-dimensional unsteady flow by the method of characteristics. The Fifth International Symposium on Detonation, Pasadena, California.

Lamb, H., 1904. On the propagation of tremors over the surface of an elastic solid. Phil. Trans. Roy. Soc. Lond. A 203, 1–42.

Lekhnitskii, S.G., 1981. Theory of elasticity of anisotropic body. Mir, Moscow, English translation.

Liu, K., Li, X., Liu, Y., 1997. Axisymmetric wave propagation in a layered transversely isotropic medium. Arch. Appl. Mech. 67, 576–588.

Liu, K., Xie, S., 1998. Two-dimensional torsional wave propagation in layered transversely isotropic cylinders. JSME Int. J. Ser. A 41, 199–203.

Luco, J.E., Apsel, R.J., 1983. On the Green's functions for a layered half-space, Part I and II. Bull. Seismol. Soc. Am. 73, 909–951.

Ting, T.C.T., 1981. Characteristic forms of differential equations for wave propagation in nonlinear media. Trans. ASME J. Appl. Mech. 48, 743–748.